Received: 6 February 2018 | Revised: 27 March 2018 | Accepted: 2 May 2018

DOI: 10.1002/ima.22277

RESEARCH ARTICLE

WILEY

No reference quality evaluation of medical image fusion

Lu Tang[1,3] | **Chuangeng Tian**[2] | **Jiansheng Qian**[3] | **Leida Li**[3]

[1] School of Medical Imaging, Xuzhou Medical University, Xuzhou, Jiangsu, China

[2] School of Information and Electrical Engineering, Xuzhou University of Technology, Xuzhou, Jiangsu, China

[3] School of Information and Control Engineering, China University of Mining and Technology, Xuzhou, Jiangsu, China

Correspondence
Leida Li, School of Information and Control Engineering, China University of Mining and Technology, Xuzhou, Jiangsu, China.
Email: lileida@cumt.edu.cn

Funding information
National Natural Science Foundation of China, Grant Number: 81771904; Natural Science Foundation of the Higher Education Institutions of Jiangsu Province, China, Grant Numbers: 17KJB416011, 16KJD320006

Abstract

Medical image fusion (MIF) attracts much attention in clinical use. Many MIF algorithms have been proposed over the past decade. Existing MIF algorithms create different fused image, however, current quality evaluation method is not designed for MIF images. So, we present a no reference quality evaluation of medical image fusion. Firstly, a MIF image database (MIFID) is built, and radiologist ratings are selected to conduct subjective test. Then an objective quality evaluation metric of medical image fusion is proposed via the phase congruency and standard deviation. Image salient features and image information are very important for visual quality of fused image. Based on this consideration, we combine the two existing quality evaluation metrics to assess MIF images. Finally, five comparative study experiments are implemented based on the MIFID. Experimental results reveal that the proposed quality evaluation metric is superior to the existing state-of-the-art metrics, which is more applicable to evaluate MIF images.

KEYWORDS

medical image fusion, no reference quality evaluation, phase congruency, standard deviation

1 | INTRODUCTION

There are many different medical imaging modalities with respective specific application in clinical diagnosis and treatment, including x-ray computed tomography (CT), magnetic resonance imaging (MRI) T1, T2 sequences, ultrasound (US), positron emission tomography (PET) and single photon emission computed tomography (SPECT). Medical image fusion (MIF) provides a promising solution approach by merging two different modality images to produce a visual enhanced fused image.[1,2] For example, by fusion of CT with MRI images, it is possible to provide dense structures and soft tissues information. Hence, a variety of MIF schemes have been widely explored by researchers in recent years. Unfortunately, quality evaluation of MIF has not been well studied. Since invariably the end user of visual information is the human observer, generally, subjective assessment is a direct and reliable method. However, subjective quality assessment is extremely slow, expensive and laborious. Some objective quality assessment studies were concerned, including DIBR-synthesized images,[3,4] multiply distorted images,[5–8] tone mapping,[9,10] screen content images,[11–13] blur images,[14] deblocked images,[15] etc. There are just a few objective evaluation metric have been presented for fused images.[16–21] Among these methods, they are designed for currency in image fusion field, not specifically for MIF. Hence, objective quality evaluation of medical image fusion is eagerly desired.

The purpose of the current work is to develop an objective quality model for MIF. Our model is inspired by phase congruency metric[16] and standard deviation metric. Phase congruency can effective capture image edges and corners salient features.[22,23] Standard deviation reflects richness of image information, which is very important in MIF.[24] Based on this consideration, an objective quality evaluation metric of medical image fusion is proposed via the phase congruency and standard deviation. Firstly, we construct a standard MIF image database (MIFID), then, radiologist ratings are selected to conduct subjective test. Finally, the capability of the

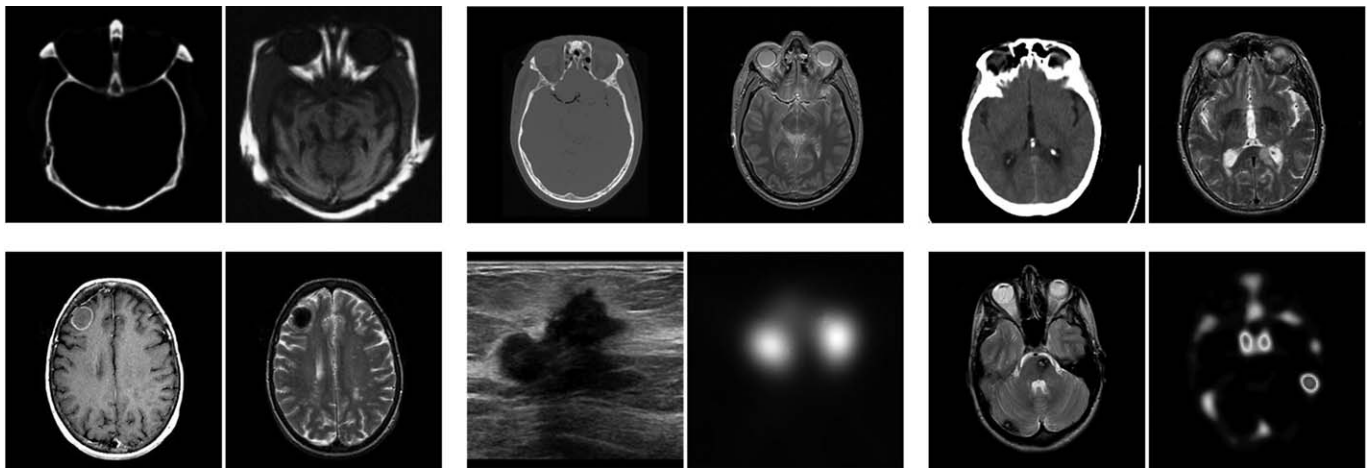

FIGURE 1 Examples of six pair input source images with different imaging modalities

proposed fusion metric is measured and five comparative study experiments are performed based on MIFID.

2 | MIF IMAGE DATABASE (MIFID)

Twenty pairs of medical images with size 256 × 256 are chosen to build the MIFID. These image pairs are selected to cover different imaging modalities. Examples of six pair input source images with different imaging modalities are shown in Figure 1. Eight MIF algorithms are used to produce 160 fused images. MIF algorithms include discrete tchebichef moments and pulse coupled neural network[1] (DTM-PCNN), nuclear norm minimization[25] (NNM), laplacian pyramid and sparse representation[24] (LP-SR), cross-scale coefficient selection[26](CSCS), guided filtering[27] (GFF), pulse coupled neural network with modified spatial frequency based on NSCT[28] (NSCT-PCNN-SF), improved sum modified laplacian[29] (ISML), convolutional sparse representation[30] (CSR), where DTM-PCNN, NNM, CSCS, NSCT-PCNN-SF, ISML and CSR are designed specifically for multimodal medical image, LP-SR and GFF are general-purpose image fusion algorithms which designed for multimodal medical image, multiexposure image, and multifocus image. In implementation, the default parameters are used. Figure 2 shows an example with one pair source image and fusion results produced by different MIF algorithms, where, (Figure 2a1-a2) denotes source image pair, (Figure 2b-i) are eight fused images. For the subjective test, twenty radiologists were required to provide a ranking score to each fused image.

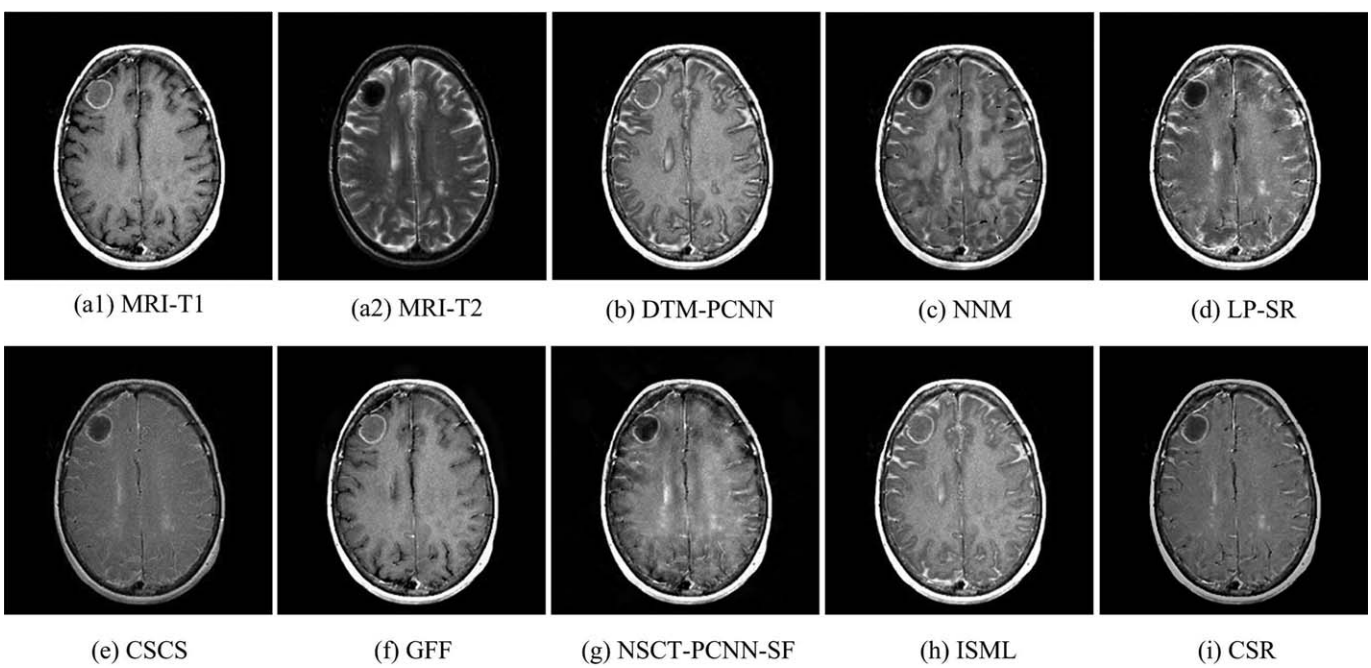

FIGURE 2 Source image pair (a1, a2) and fusion results (b)-(i) produced by different MIF algorithms

They are in the range [1, 5]. For each fused image, subjective scores and standard deviation are computed and denoted by

$$\bar{u} = \frac{1}{T}\sum_{i=1}^{T} u_i \tag{1}$$

$$\sigma = \sqrt{\sum_{i=1}^{T} \frac{(u_i - \bar{u})^2}{(T-1)}} \tag{2}$$

where u_i denotes the subjective score of the ith radiologists, T stands for the number of radiologists ($T = 20$). Subjective scores are also called mean opinion score (MOS).

The performances are assessed based on two commonly evaluation criteria,[31–33] namely spearman rank-order correlation coefficient (SRCC) and kendall rank-order correlation coefficient (KRCC). Their range is [0, 1]. Both SRCC and KRCC are nonparametric rank-order based correlation metric, independent of any monotonic nonlinear mapping between subjective and objective scores, which are defined as

$$SRCC = 1 - \frac{6\sum_{j=1}^{N} d_j^2}{N(N^2-1)} \tag{3}$$

$$KRCC = \frac{N_c - N_d}{1/2(N(N-1))} \tag{4}$$

where d_j denotes the difference between the jth image's ranks between subjective and objective evaluations. N_c and N_d are the numbers of concordant (of consistent rank order) and discordant (of inconsistent rank order) pairs in the data set, respectively.

Table 1 shows the subjective scores of SRCC and KRCC performance over all subjects together with the corresponding standard deviations. The average KRCC and SRCC values are displayed in the last line. From Table 1, we can see that each individual subject range from 0.7 to 0.9, however, corresponding standard deviation is no more than 0.16, which indicates that the scope is concentrated and the difference is not significant. So, subjective performance is quite consistent, with relatively low changes.

TABLE 1 KRCC and SRCC values of subject

	SRCC		KRCC	
Image set	**μ(subject)**	**σ(subject)**	**μ(subject)**	**σ(subject)**
1	0.7385	0.1030	0.8440	0.0752
2	0.8059	0.0817	0.8967	0.0534
3	0.7718	0.1207	0.8732	0.0967
4	0.7244	0.1104	0.8298	0.0833
5	0.7219	0.0908	0.8360	0.0651
6	0.7941	0.0951	0.8917	0.0599
7	0.7907	0.0966	0.8914	0.0625
8	0.7549	0.1050	0.8616	0.0845
9	0.7919	0.0955	0.8759	0.0761
10	0.7741	0.1055	0.8726	0.0782
11	0.7890	0.1042	0.8810	0.0795
12	0.7965	0.0979	0.8827	0.0719
13	0.7908	0.1046	0.8771	0.0710
14	0.8007	0.1196	0.8935	0.0804
15	0.7816	0.1244	0.8726	0.0932
16	0.7499	0.1289	0.8548	0.1003
17	0.7728	0.1546	0.8637	0.1329
18	0.7821	0.0953	0.8747	0.0739
19	0.7682	0.1234	0.8783	0.0780
20	0.8122	0.0868	0.8997	0.0590
Average	0.7756	0.1072	0.8726	0.0788

3 | OBJECTIVE QUALITY EVALUATION METRIC

Following the phase congruency and standard deviation, we found image salient features and image information are very important for visual quality of MIF image. Based on this consideration, we combine the two existing quality evaluation to assess MIF images.

3.1 | Phase congruency

Phase congruency provides brightness and contrast invariant feature extraction. There are several benefits. First, when the object is same, the images also obtained in different modalities have obviously different pixel maps. The phase consistency is the same as different pixel intensity maps. Second, different modalities of capture environment vary, resulting in light and contrast changes. Third, image salient features edges and corners are confirmed via collecting the frequency parts in the phase. The phase congruency gives the largest phase of the fourier component, and supplies the improved location of the image features.[34,35] Inspired by these main properties, phase congruency is used to evaluate the MIF. Q_p based on phase congruency measurement[16] is given by

$$Q_p = (P_p)^{\alpha}(P_M)^{\beta}(P_m)^{\gamma}, \tag{5}$$

where P_p, P_M, P_m will be obtained from two input images, respectively. These three values are defined as the maximum one of C_{xy}^k:

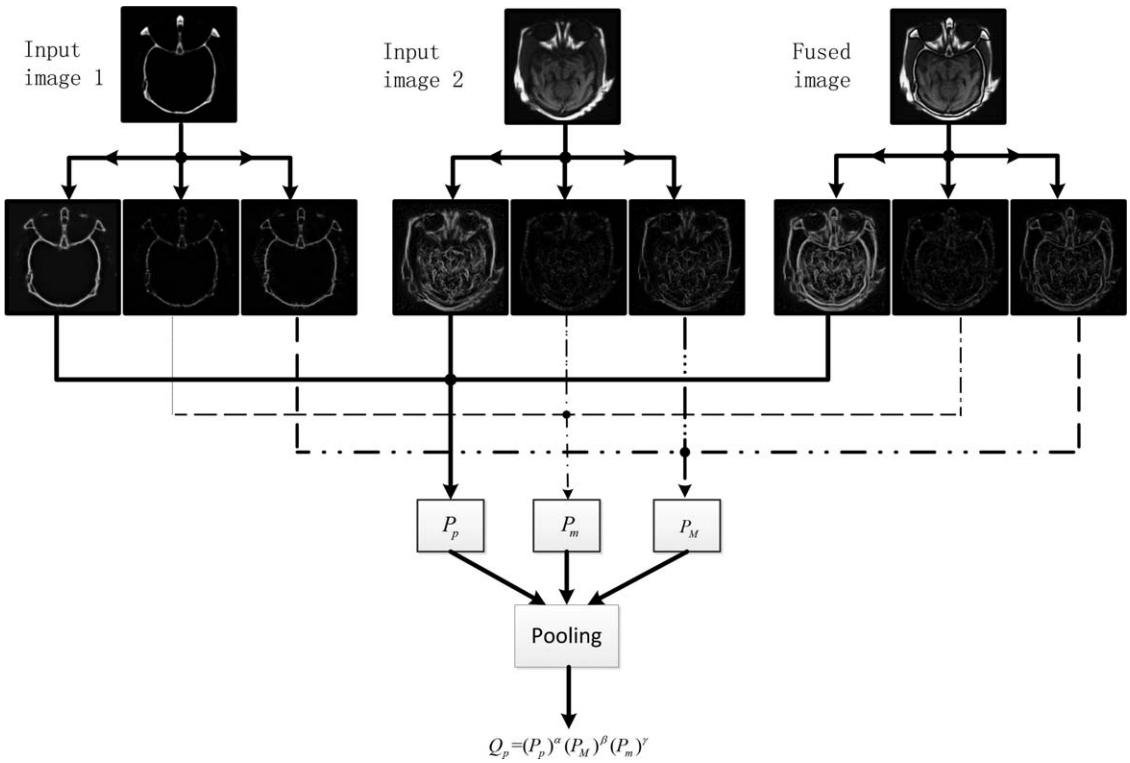

FIGURE 3 Example of phase congruency evaluation metric

$$P_p=\max\left(C_{1f}^{P}, C_{2f}^{P}, C_{mf}^{P}\right), \tag{6}$$

$$P_M=\max\left(C_{1f}^{M}, C_{2f}^{M}, C_{mf}^{M}\right), \tag{7}$$

$$P_m=\max\left(C_{1f}^{m}, C_{2f}^{m}, C_{mf}^{m}\right), \tag{8}$$

and there is

$$C_{xy}^{k}=\frac{\sigma_{xy}^{k}+C_k}{\sigma_x^{k}\sigma_y^{k}+C_k}, \tag{9}$$

C_{xy}^{k} represents the correlation coefficients between the two groups of x and y. $\{k|P,M,m\}$ stands for the phase congruency map and corresponding principal moments. That also k equivalent to *P, M or m*. 1, 2, m refer the two input images with different imaging modalities and their corresponding selected maximum map, f is the result obtained from the fused medical image. α, β, γ are adjusted by three parts. In this article, the small constant value C_k is selected as 0.0001, and $\alpha=1,\beta=1,\gamma=1$ by experiments. Figure 3 shows the example of phase congruency evaluation metric.

3.2 | Standard deviation

Metric based standard deviation (Q_{SD}) calculates the sharpness and clarity of MIF image. The larger value indicates a better degree of closeness with the original image. SD[24] demonstrates the overall active level of fused image and their high values depict fine details of the image, such as contours and edges. The Q_{SD} of the fused image is defined as

$$Q_{SD}=\sqrt{\frac{1}{N\times M}\sum_{x=1}^{N}\sum_{y=1}^{M}(F(x,y)-\mu)^2}, \tag{10}$$

where the size of input source image is denoted by $N\times M$, F represents the medical fusion image and μ is the mean value of F.

3.3 | Overall quality evaluation

The phase congruencyQ_p and standard deviation Q_{SD} measure introduced above characterize different aspects of MIF images quality. The final overall quality score of fused image is computed by polling them as

$$Q=a(Q_p)^b+(1-a)(Q_{SD})^c \tag{11}$$

where three parameters a,b,c are adjusted to balance the relative relationship between the two parts to evaluate MIF images based on MIFID. In implementation, we use for loop to optimize parameters, we get the results of $a=0.2,b=1,c=1$ after pooling in average result of overall quality score are best. In this article, we set $a=0.2,b=1,c=1$ by experiments.

4 | EXPERIMENTAL AND ANALYSES

To confirm validity of the presented fusion quality metric, Q_p, Q_{SD} are combined to evaluate the MIF with Equation 11 and test their performances based on MIFID. Table 2 shows

TABLE 2 Performance assessment of proposed metric and its two components

Image set	SRCC			KRCC		
	Q_p	Q_{SD}	Pooling	Q_p	Q_{SD}	Pooling
1	0.9762	0.8333	0.8810	0.9286	0.6429	0.7143
2	0.7143	0.4286	0.5714	0.5714	0.4286	0.5000
3	0.3095	0.7381	0.8095	0.2143	0.6429	0.7143
4	0.0714	0.5714	0.8095	0.2546	0.4286	0.6429
5	0.2857	0.7619	0.9048	0.2143	0.6429	0.7857
6	0.1190	0.7381	0.8095	0.0714	0.5000	0.6429
7	0.0238	0.5952	0.7857	0.2857	0.4286	0.6429
8	0.3333	0.4286	0.5476	0.0156	0.3571	0.4286
9	0.4048	0.7619	0.8810	0.3571	0.5714	0.7143
10	0.4048	0.6190	0.7381	0.3571	0.5714	0.6429
11	0.5714	0.6905	0.7381	0.5000	0.5714	0.6429
12	0.2798	0.9222	0.9701	0.1818	0.8365	0.9092
13	0.0714	0.7319	0.9515	0.0378	0.6425	0.8693
14	0.4286	0.0238	0.3095	0.2857	0.0112	0.2857
15	0.6131	0.8144	0.9701	0.4286	0.6910	0.9092
16	0.0476	0.7619	0.7857	0.2143	0.5429	0.6429
17	0.1190	0.8810	0.9048	0.0714	0.7143	0.7857
18	0.0161	0.8095	0.9048	0.2143	0.6429	0.7857
19	0.0714	0.7143	0.8571	0.1429	0.5714	0.7143
20	0.3095	0.8001	0.8333	0.2857	0.6143	0.7143
Average	0.3085	0.6813	0.7982	0.2816	0.5526	0.6844

TABLE 3 SRCC values of five image fusion quality metrics and the proposed metric on MIFID

Image set	SRCC					
	Q_G	Q_S	Q_E	Q_{RSFE}	Q_{MI}	Proposed
1	0.7619	0.8810	**0.9762**	0.5952	0.1429	0.8810
2	0.4048	0.3571	0.5476	0.0476	0.2381	**0.5714**
3	0.5952	0.5714	0.4286	0.0714	0.2857	**0.8095**
4	0.7143	0.7857	0.2857	0.1905	0.5238	**0.8311**
5	0.7143	0.8095	0.4286	0.0952	0.6667	**0.9048**
6	0.3095	0.3810	0.3810	0.3810	0.1190	**0.8095**
7	0.4524	0.6190	0.5000	0.3810	0.2857	**0.7857**
8	0.1667	0.3333	0.3810	0.5000	0.0171	**0.5476**
9	0.0714	0.6190	0.3095	0.2619	0.2857	**0.8799**
10	0.5000	0.5714	0.5000	**0.8095**	0.6429	0.7381
11	0.1429	0.0714	0.2619	0.2143	0.3810	**0.7231**
12	0.6845	0.6845	0.8036	0.7083	0.6845	**0.9701**
13	0.7857	0.9048	0.5714	0.5952	0.6667	**0.9515**
14	0.5952	0.4048	**0.7619**	0.3810	0.2619	0.3095
15	0.8988	0.9226	0.7917	0.2202	0.4821	**0.9701**
16	0.6190	0.5952	0.1905	0.2857	**0.8810**	0.7857
17	0.8571	0.8095	0.8333	0.8571	0.8571	**0.9048**
18	0.4048	0.6429	0.0714	0.3095	0.8810	**0.9016**
19	0.2143	0.5476	0.0476	0.2381	0.7619	**0.8571**
20	**0.9048**	0.7857	0.7381	0.6429	0.7619	0.8333
Average	0.5399	0.6149	0.4905	0.3893	0.4913	**0.7982**

the performances of each component (Q_p, Q_{SD}), and proposed metric in terms of both KRCC and SRCC, including the results of every fused image set, along with the average values for all fused image sets. It is observed from Table 2 that two components provide significant positive correlations with subjective opinions, Q_{SD} exhibits major contribution, while the overall quality delivers substantial and consistent performance improve over two components. Since two components are upper-bounded by 1, the overall quality score is also upper-bounded by 1, which corresponds to perfect contrast preservation, sharpness simultaneously.

To further validate effectiveness of the presented quality module, our measure is also compared with the existing image fusion quality measures, including: Gradient-based fusion metric[17] (Q_G), Structure-based metrics[18] (Q_S), Edge information[19] (Q_E), Ratio of spatial frequency error based metrics[20] (Q_{RSFE}), Mutual information based metrics[21] (Q_{MI}). Tables 3 and 4 summarize the KRCC and SRCC performance of all 20 image sets for all five image fusion quality metrics, and the best scores are marked in blackbody. In general, the larger the values of SRCC, KRCC indicate better quality evaluation metric. SRCC is a nonparametric rank-order based correlation metric, independent of any monotonic nonlinear mapping between subjective and objective scores. KRCC is another nonparametric rank correlation metric. In Many objective quality assessment metrics,[3–15] authors also used this statistical analysis. However, in the state-of-the-art fusion quality measures, such as Q_G, Q_S, Q_E, Q_{RSFE}, Q_{MI}, authors have not been done to compare them with subjective data that contain a wide variety of image modalities and fusion algorithms. So, the proposed quality assessment metric is tested based on the MIF database.

TABLE 4 KRCC values of five image fusion quality metrics and the proposed metric on MIFID

Image set	KRCC					
	Q_G	Q_S	Q_E	Q_{RSFE}	Q_{MI}	Proposed
1	0.5714	0.7143	**0.9286**	0.5000	0.1429	0.7143
2	0.2857	0.2143	0.4286	0.1121	0.2143	**0.5000**
3	0.4286	0.5000	0.2857	0.0714	0.2143	**0.7143**
4	0.4728	0.6183	0.0364	0.1091	0.3273	**0.6429**
5	0.5714	0.6429	0.3571	0.0136	0.5714	**0.7857**
6	0.1429	0.2143	0.2857	0.2857	0.0714	**0.6430**
7	0.3571	0.4286	0.2143	**0.6429**	0.2857	**0.6429**
8	0.2857	0.4286	0.0714	**0.5000**	0.2857	0.4286
9	0.0714	0.4286	0.2143	0.2857	0.0714	**0.7144**
10	0.3571	0.5000	0.3571	**0.7143**	0.4286	0.6428
11	0.0714	0.0714	0.2857	0.0121	0.3571	**0.6429**
12	0.5455	0.5456	0.6910	0.5455	0.5455	**0.9092**
13	0.6425	0.7937	0.4921	0.4956	0.4914	**0.8693**
14	0.2857	0.2143	**0.5714**	0.1429	0.3571	0.2857
15	0.7143	0.7857	0.5714	0.0714	0.2857	**0.9092**
16	0.2857	0.2857	0.1429	0.0714	0.5714	**0.6429**
17	0.7143	0.5714	0.6429	0.6429	0.7143	**0.7857**
18	0.2143	0.2857	0.1429	0.1429	0.6429	**0.7836**
19	0.1311	0.1519	0.2143	0.1429	0.4286	**0.7143**
20	**0.7857**	0.6429	0.5714	0.5000	0.5714	0.7101
Average	0.3967	0.4519	0.3753	0.3001	0.3789	**0.6841**

Tables 3 and 4 show that the presented scheme performs the best results on the average in both KRCC and SRCC. The existing image fusion quality methods seem unable to supply enough quality for the prediction of MIF images.

5 | CONCLUSION

MIF attracts much attention in clinical use because of clinical diagnosis and treatment. However, current quality evaluation method is not designed for MIF images. In this article, we present a no reference quality evaluation metric of medical image fusion via combining phase congruency and standard deviation. We have built a MIFID, and subjective test is implemented to select the radiologist ratings. To confirm validity of the presented fusion quality metric, five comparative study experiments are implemented based on the MIFID. Experimental results show that proposed metric is superior to the existing state-of-the-art metrics, which is more applicable to evaluate MIF images.

ACKNOWLEDGMENT

This work was supported by the National Natural Science Foundation of China (No.81771904), Natural Science Foundation of the Higher Education Institutions of Jiangsu Province, China (17KJB416011, 16KJD320006).

ORCID

Lu Tang http://orcid.org/0000-0003-0354-185X

REFERENCES

[1] Tang L, Qian JS, Li LD, Hu JF, Wu X. Multimodal medical image fusion based on discrete tchebichef moments and pulse coupled neural network. *Int J Imaging Syst Technol.* 2017; 27: 57–65.

[2] Qian J, Bao R, Shen W, Hu J, Tang L, Xia Z. Perceptual medical image fusion with internal generative mechanism. *Electron Lett.* 2017; 53:1184–1186.

[3] Gu K, Jakhetiya V, Qiao JF, Li XL, Lin WS, Thalmann D. Model-based referenceless quality metric of 3D synthesized images using local image description. *IEEE Trans Image Process* 2018; 27:394–405.

[4] Li L, Zhou Y, Gu K, Lin W, Wang S. Quality assessment of DIBR-synthesized images by measuring local geometric distortions and global sharpness. *IEEE Trans Multimedia.* 2018; 20: 914–926.

[5] Gu K, Zhai G, Lin W, Yang X, Zhang W. Visual saliency detection with free energy theory. *IEEE Signal Process Lett.* 2015; 22:1552–1555.

[6] Gu K, Zhai G, Yang X. Hybrid no-reference quality metric for singly and multiply distorted images. *IEEE Trans Broadcast.* 2014; 60:555–567.

[7] Yue G, Hou C, Gu K, et al. Analysis of structural characteristics for quality assessment of multiply distorted images. *IEEE Trans Multimedia.* 2018; https://doi.org/10.1109/TMM.2018.2807589.

[8] Gu K, Zhai G, Yang X, Zhang W. A new psychovisual paradigm for image quality assessment: from differentiating distortion types to discriminating quality conditions. *Signal Image Video Process.* 2013; 7:423–436.

[9] Yue G, Hou C, Gu K, Mao S, Zhang W. Biologically inspired blind quality assessment of tone-mapped images. *IEEE Trans Ind Electron.* 2018; 65:2525–2536.

[10] Yeganeh H, Wang Z. Objective quality assessment of tone-mapped images. *IEEE Trans Image Process.* 2013; 22:657–667.

[11] Gu K, Zhou J, Qiao JF, Zhai GT, Lin WS, Bovik AC. No-reference quality assessment of screen content pictures. *IEEE Trans Image Process* 2017; 26:4005–4018.

[12] Wang SQ, Gu K, Zhang X, Lin W, Ma S, Gao W. Reduced-reference quality assessment of screen content images. *IEEE Trans Circ Syst Video Technol.* 2018; 28:1–14.

[13] Fang Y, Yan J, Li L, Wu J, Lin W. No reference quality assessment for screen content images with both local and global feature representation. *IEEE Trans Image Process.* 2018; 27:1600–1610.

[14] Yue G, Hou C, Gu K, Ling N. No reference image blurriness assessment with local binary patterns. *J Vis Commun Image Represent.* 2017; 49: 382–391.

[15] Li L, Zhou Y, Lin W, Wu J, Zhang X, Chen B. No-reference quality assessment of deblocked images. *Neurocomputing.* 2016; 177:572–584.

[16] Zhao J, Laganiere R, Liu Z. Performance assessment of combinative pixel-level image fusion based on an absolute feature measurement. *Int J Innovative Comput Inf Control.* 2007; 3: 1433–1447.

[17] Xydeas CS, Petrovic VS. Objective image fusion performance measure. *Electron Lett.* 2000; 36:308–309.

[18] Yang C, Zhang J-Q, Wang X-R, Liu X. A novel similarity based quality metric for image fusion. *Inf Fusion.* 2008; 9:156–160.

[19] Li S, Kwok JT, Wang Y. Combination of images with diverse focuses using the spatial frequency. *Inf Fusion.* 2001; 2:169–176.

[20] Zheng Y, Essock EA, Hansen BC, Haun AM. A new metric based on extended spatial frequency and its application to DWT based fusion algorithms. *Inf Fusion.* 2007; 8:177–192.

[21] Qu G, Zhang D, Yan P. Information measure for performance of image fusion. *Electron Lett.* 2002; 38313–315.

[22] Kovesi P. Image features from phase congruency. *J Comput Vision Res.* 1999; 1:2–26.

[23] Kovesi P. Phase congruency: A low-level image invariant. *Psychol Res.* 2000; 64:136–148.

[24] Liu Y, Liu S, Wang Z. A general framework for image fusion based on multi-scale transform and sparse representation. *Inf Fusion.* 2015; 24:147–164.

[25] Liu SQ, Zhang T, Li HL, Zhao J, Li HY. Medical image fusion based on nuclear norm minimization. *Int J Imaging Syst Technol.* 2015; 25:310–316.

[26] Shen R, Cheng I, Basu A. Cross-scale coefficient selection for volumetric medical image fusion. *IEEE Trans Biomed Eng.* 2013; 60:1069–1079.

[27] Li S, Kang X, Hu J. Image fusion with guided filtering. *IEEE Trans Image Process.* 2013; 22:2864–2875.

[28] Das S, Kundu MK. NSCT-based Multimodal medical image fusion using pulse-coupled neural network and modified spatial frequency. *Med Biol Eng Comput.* 2012; 50:1105–1114.

[29] Liu S, Zhao J, Shi M. Medical image fusion based on improved sum-modified-Laplacian. *Int J Imaging Syst Technol* 2015; 25: 206–212.

[30] Liu Y, Chen X, Ward RK, Jane Wang Z. Image fusion with convolutional sparse representation. *IEEE Signal Process Lett.* 2016; 23:1882–1886.

[31] Li LD, Lin WS, Wang XS, Yang GB, Bahrami K, Kot AC. No reference image blur assessment based on discrete orthogonal moments. *IEEE Trans Cybern.* 2016; 46:39–50.

[32] Li LD, Zhu HC, Yang GB, Qian JS. Referenceless measure of blocking artifacts by Tchebichef kernel analysis. *IEEE Signal Process Lett.* 2014; 21:122–125.

[33] Hassen R, Wang Z, Salama MM. Objective quality assessment for multiexposure multifocus image fusion. *IEEE Trans Image Process.* 2015; 24:2712–2724.

[34] Bhatnagar G, Wu QMJ, Liu Z. Directive contrast based multimodal medical image fusion in NSCT domain. *IEEE Trans Multimedia.* 2013; 15:1014–1024.

[35] Bhatnagar G, Wu QMJ, Liu Z. A new contrast based multimodal medical image fusion framework. *Neurocomputing.* 2015; 157: 143–152.

How to cite this article: Tang L, Tian C, Qian J, Li L. No reference quality evaluation of medical image fusion. *Int J Imaging Syst Technol*. 2018;00:1–7. https://doi.org/10.1002/ima.22277